MONITORING AND ANALYSIS OF LANDSLIDE HAZARD USING DINSAR TECHNIQUE APPLIED TO ALOS PALSAR IMAGERY: A CASE STUDY IN KAYANGAN CATCHMENT AREA, YOGYAKARTA, INDONESIA

Ratih Fitria Putri[1*], Sunu Wibirama[2], Ilham Alimuddin[3], Hiroaki Kuze[1,4] and Josaphat Tetuko Sri Sumantyo[1,4]

[1]Graduate School of Advanced Integration Science, Chiba University, Chiba, 263-8522, Japan
[2]Department of Electrical Engineering, Faculty of Engineering, Gadjah Mada University,Yogyakarta, 55281, Indonesia
[3]Department of Geology, Faculty of Engineering, Hasanuddin University, Makasar, 9024, Indonesia
[4]Center for Environmental Remote Sensing (CEReS), Chiba University, 263-8522, Japan

Abstract: The differential synthetic aperture radar interferometry (DInSAR) technique is applied to the ALOS PALSAR data to observe surface displacement in Kayangan catchment area, Yogyakarta, Indonesia. Change detection is implemented to extract information on several landslides that occurred in the region in a time span between 2007 and 2009. The advanced DInSAR processing of images (2007–2009) has shown slight surface movements before the landslide events. These results are compared and validated with available GPS measurements. Our analysis reveals that Kayangan catchment area exhibits clear indication of surface displacements varying from 5.2 to 57.9 cm/year. The occurence of landslides has been analyzed in relation to the following terrain parameters; elevation, slope, distance to stream network, geology, landuse, and distance from road. Among these factors, it is found that 18% of landslides occur in elevation >100 m, 56% in slope 30–40°, 34% in <25 m distance to stream networks, 100% in kebobutak formation, 67% in mix garden of land use types, and 100% in <25 m distance from road. The landuse is the most influential factor, since there are only four types of landuse that can lead to landslide occurrence, i.e., mixed garden, dryland agriculture, bush, and settlement. The analysis of land deformation is promising for assessing acceleration caused by a destabilizing anthropogenic change, and relationship between seasonal precipitation and deformation variability.

---

[1] Correspondence to: Ratih Fitria Putri. E-mail: ratihfp@chiba-u.jp.

INTRODUCTION

Disasters, both natural and man-made, are increasing in their frequency and catastrophic impact in Indonesia. Natural hazards such as landslides, avalanches, floods and debris flows can result in enormous property damage and human casualties in mountainous regions (Matternich *et al.*, 2005). Earthquake, flood, landslide, subsidence are only a few to mention (Walter *et al.*, 2008, Abidin *et al.*, 2008, Chini *et al.*, 2008, US. Geology Survey, 2006, Tsuji *et al.*, 2009). Due to the lack or inadequate disaster prevention and mitigation strategies, the impact of such disasters is much greater in Indonesia than in other developed countries. Disaster detection and monitoring are essential aspects in disaster mitigation. Although detection and monitoring processes are conventionally performed by ground survey, it is often difficult to assess the damage correctly, especially when wide area coverage has to be targeted.

Satellite remote sensing is a technology that can be exploited for producing images indispensable for gathering pertinent information on wide area disasters (Matternicht *et al.,* 2005). Active microwave remote sensing, in particular, has been proven to be suitable for disaster monitoring, because of the availability of images for both daytime and nighttime regardless of cloud coverage. The ability of synthetic aperture radar (SAR) to provide high resolution images in all weather conditions gives advantages in tropical regions, where the presence of clouds often hinders the application of optical remote sensing. In the past decades, SAR has been widely used in environmental monitoring, earth-resource mapping, and disaster mapping (Massonet *et al.*, 1993, Ozawa *et al.*, 1997, Rosen *et al.*, 1999, Dong *et al.*, 2010).

By analyzing SAR data, geometrically accurate imagery can be generated with medium to high spatial resolution. Moreover, the use of coherency of microwave signal enables one to detect topographical and deformation changes by processing the signal phase. This creates the basis for the interferometry SAR (InSAR) and differential interferometry SAR (DinSAR) techniques. DInSAR, as well as advanced DInSAR, is a powerful technique for detecting and measuring land
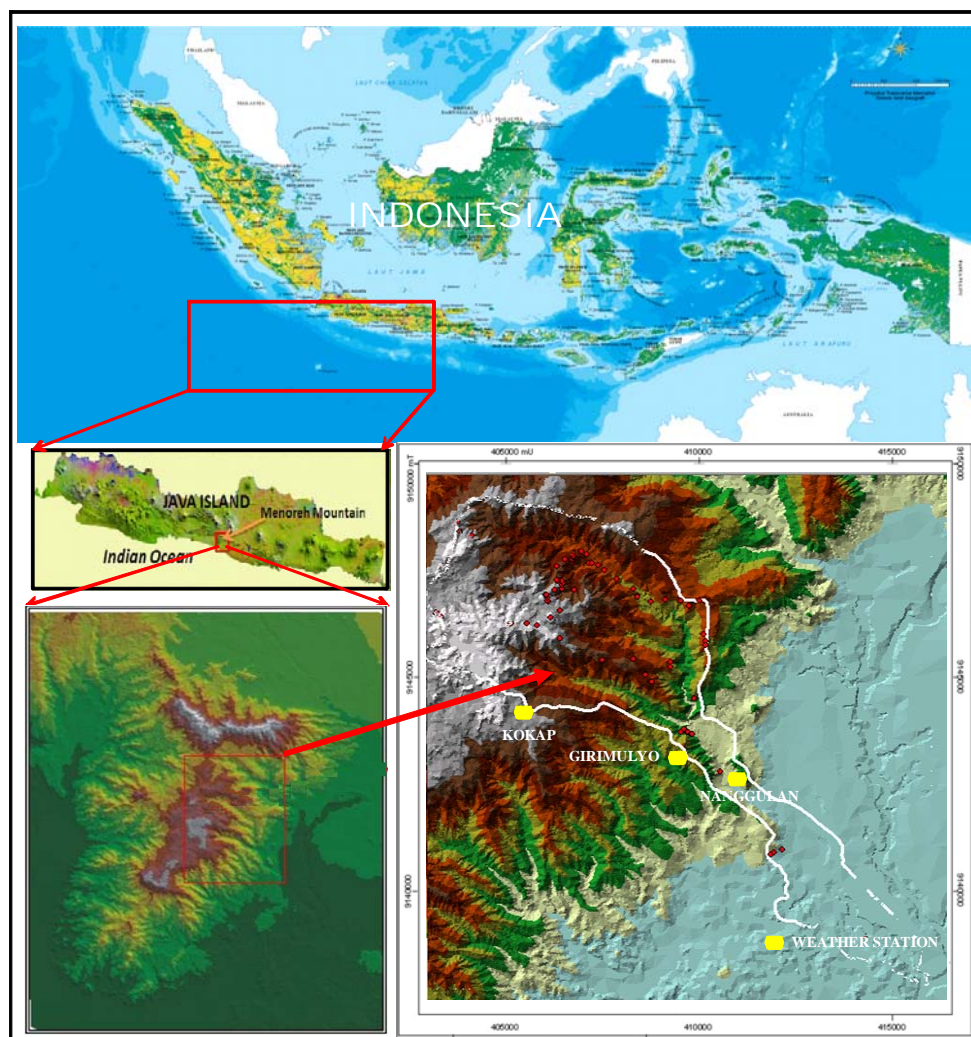

Fig. 1 Location of study area: Kayangan catchment, Yogyakarta, Indonesia.

surface displacement from space over wide areas. The advantages and limitations of conventional DInSAR for the periodical survey of slope movements were investigated by Rott *et al.* (1999) and Squarzoni *et al.* (2003). Advanced DInSAR techniques compute displacement time series using large sequences of SAR images. The results presented in several papers have proven the practicality of advanced DInSAR exploitation for landslides monitoring and analysis (Strozzi *et al.,* 2005, Riedel *et al.,* 2008, Putri *et al.*, 2013).

The phased array type L-band SAR (PALSAR) was launched in 2006 onboard the advanced land observing satellite (ALOS) (Rosenqvist *et al.,* 2007). In the present paper, the DInSAR analysis is implemented on ALOS PALSAR data from 2007 to 2009 to detect landslide events in Kayangan catchment area, Yogyakarta Province, Indonesia (**Fig. 1**). In this

considered as highly vulnerable areas (Ignasius *et al.*, 2012). Regional statistics (BPS, 2008) show that about 88% are living in rural areas and 78% households are working in agricultural sector. Although a significant portion of the landslides occurred after heavy precipitation, multiple factors, both natural and anthropogenic, are closely related to the events. Fluvial erosion, excavation, and enhanced infiltration were among such causes, as suggested from the study of landslides in Kayangan catchment by using geographic information system (GIS) data of lithological map and digital elevation model (DEM) (Hadmoko *et al.*, 2008, Ignasius and Nursa'ban, 2012). To the best of the present authors' knowledge, the application of ALOS PALSAR data to detect landslides in Kayangan catchment area has never been reported in previous literatures. In this paper, we suggest a new approach to analyze surface displacements due to landslides in
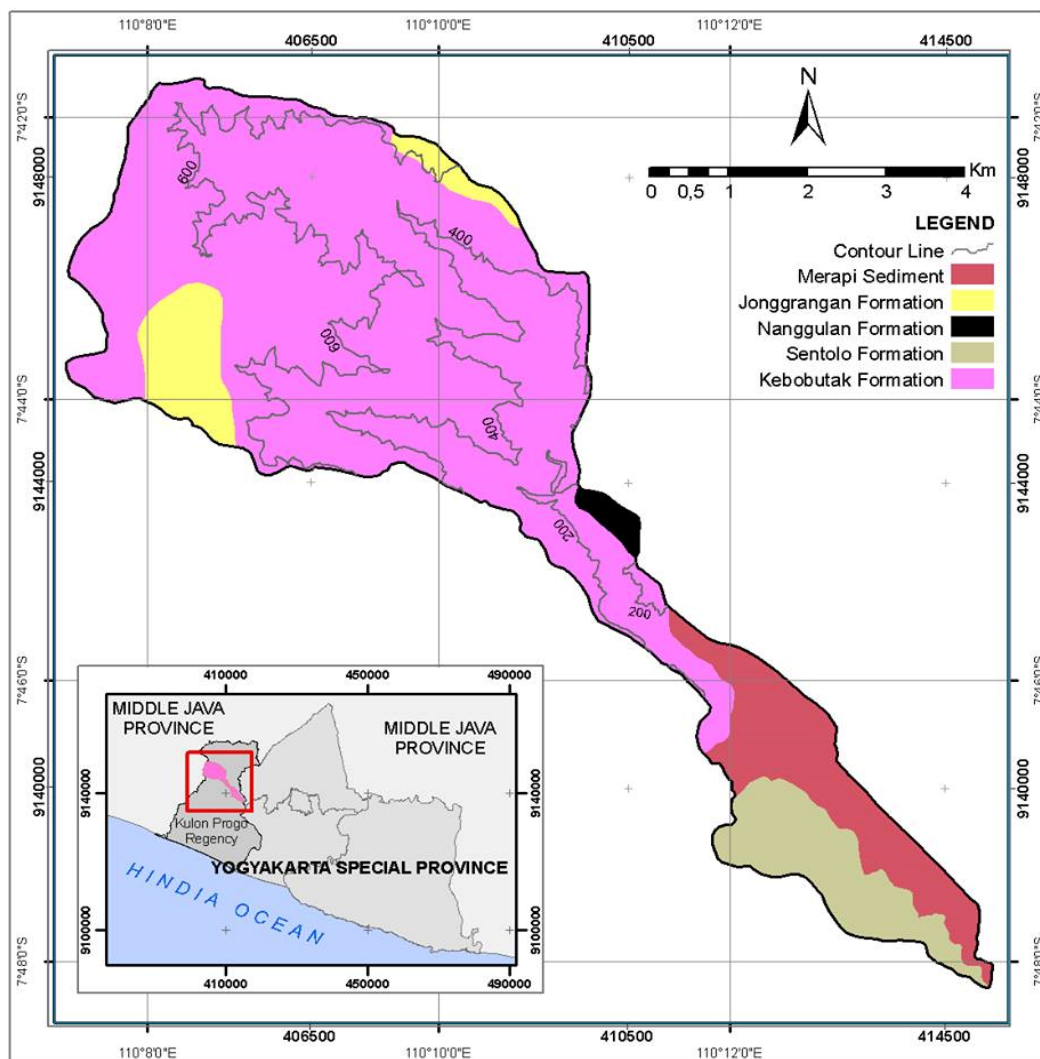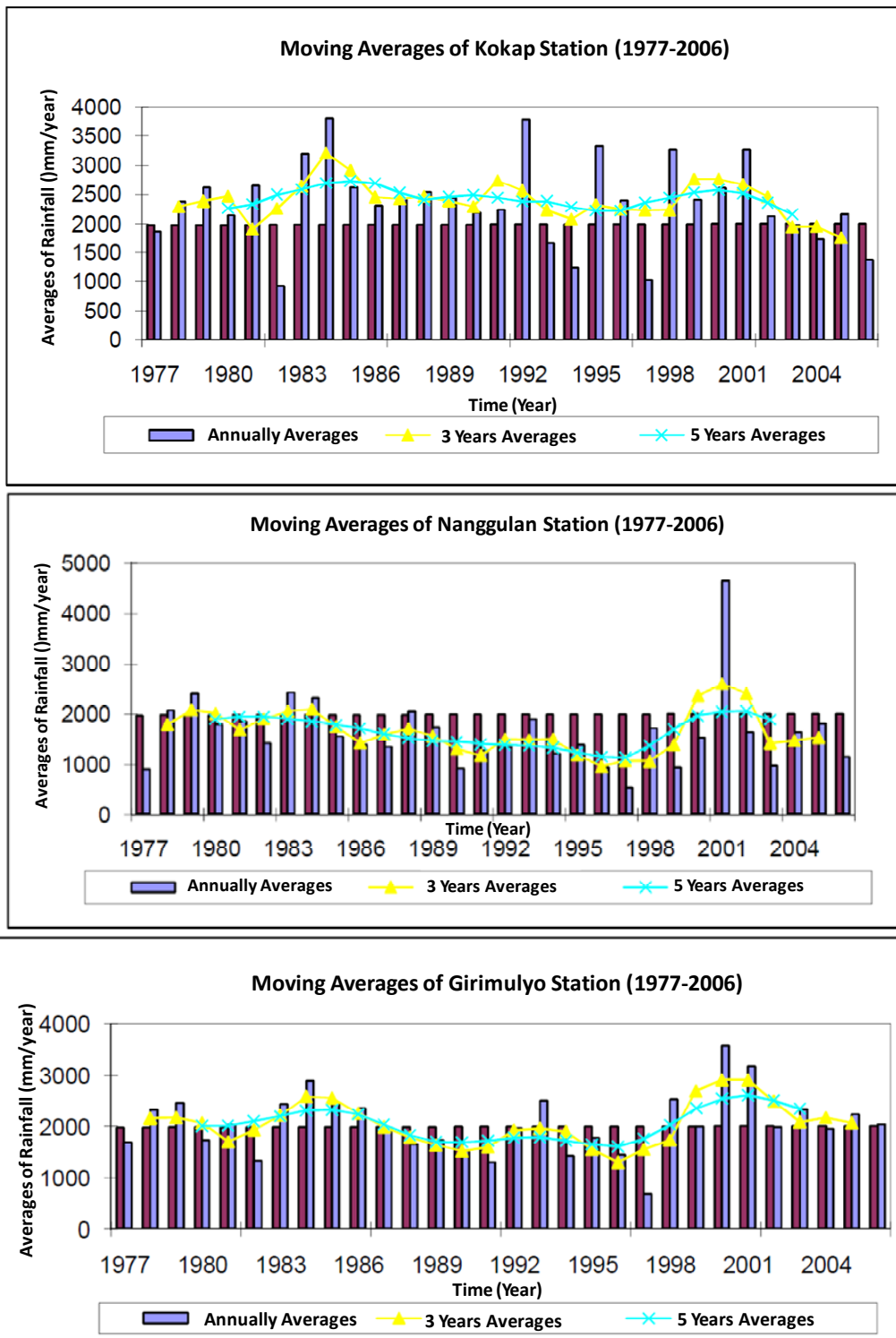

Fig. 2 Geology Map of Kayangan catchment, Indonesia.

catchment, approximately 1211 ha (49.6%) is

Kayangan catchment by using DInSAR processing of

Moving Averages of Kokap Station (1977-2006)

Moving Averages of Nanggulan Station (1977-2006)

Moving Averages of Girimulyo Station (1977-2006)

ALOS PALSAR data. The result of satellite analysis is compared with our ground survey data obtained in 2013 to confirm the reliability of the proposed method. We discuss the advantages and limitations of advanced DInSAR processing on ALOS PALSAR imaginary. It is found that the DInSAR technique is able to map slight surface deformation for a specific type of landslides.

Study Area

The study area covers the whole Kayangan catchment in Kulon Progo in Yogyakarta Province (**Fig. 1**). Kayangan catchment is geographically located at 7°41′24″–7°48′00″ and 110°07′12″–110°13′48″. The catchment area has complex terrain characteristics with elevation of 49–825 m (Hadmoko *et al.*, 2008). Also, the geological condition is complex, with some major faults in the middle part of the present study area. Geologically, the area consists of five formations (see **Fig. 2**), i.e., Nanggulan formation (sandstone with intercalated of lignited, sandy marl, claystone with

limonite concretion, intercalation of marl, sandstone and tuff), Kebobutak formation (andesitic breccias, tuff, lapilli tuff, aggromelare and andesitic lava flows), Jonggrangan formation (conglomerate, tuffaceous marl and calcareous sandstone, limestone, and coralline limestone), old andesit, colluviums; and alluvium Sentolo formation (limestone and marly sandstone) (Rahardjo *et al.*, 2005). The geodynamic behavior is relatively dynamic and approximated by several major faults encompassing the catchment area.

Kayangan catchment has humid tropical climate characteristics. Because of strong orographic effect, annual precipitation is extremely variable, ranging from about 2500 to nearly 4000 mm/year (**Fig. 3**). Kayangan catchment has been experiencing landslide hazard in certain areas in which heavy rainfall occurred before a landslide event. Climate conditions in this area are determined by rainfall, wind and temperature. Due to wet tropical climate with a relatively high temperature environment, denudational processes such as weathering, erosion and landslide are very intensive in most lithological settings (Hadmoko *et al.*, 2008). Zaruba & Mencl (1982) pointed out a strong relationship between the landslide with the intensity and duration of rainfall in a region. Weather monitoring stations around the river basin that can be used to retrieve weather data in the watershed include Girimulyo, Kokap and Nanggulan stations.

Our field observations have shown that typical landslide types in Kayangan catchment are slump and transitional slide as depicted in **Fig. 4**. The transitional slide is often seen in rock layers and the material moves down a bedding plane or layer. Slump type has

Table 1. ALOS PALSAR image pairs and baseline information

Data Acquisition (RSP 432)		Baseline (m)	Perpendicular Baseline (m)	Temporal Baseline (week)
Master	Slave			
12/05/2008	10/08/2007	-149.12	-567.00	36
12/08/2008	10/08/2007	284.12	230.14	48
12/08/2008	12/05/2008	433.05	796.98,	12
15/08/2009	10/08/2007	328.51	92.19	96
15/08/2009	12/05/2008	477.50	659.10	60
15/08/2009	12/08/2008	44.49	-137.76	48

seen in unconsolidated material. No mixing takes place in the slump mass, and scarps are formed at the top of the sliding site.

DATA AND METHODOLOGY

ALOS PALSAR Data

The ALOSPALSAR was designed to achieve high performance and flexibility with the L-band operation, following its predecessor, the Japanese Earth Resources Satellite-1 (JERS-1). Active phased array antenna equipment provides variable incidence angle ranging from 8 to 50 degrees, allowing the ScanSAR operation. In order to visually identify areas affected by landslides, we utilize the PALSAR images. Pairs of images acquired on 20 August 2007, 12 May 2008, 12 August 2008 and 15 August 2008 are used here to compare the pre-event and post-event situations of the Kayangan catchment landslides. The data have the same observation parameters of center frame number 7020,
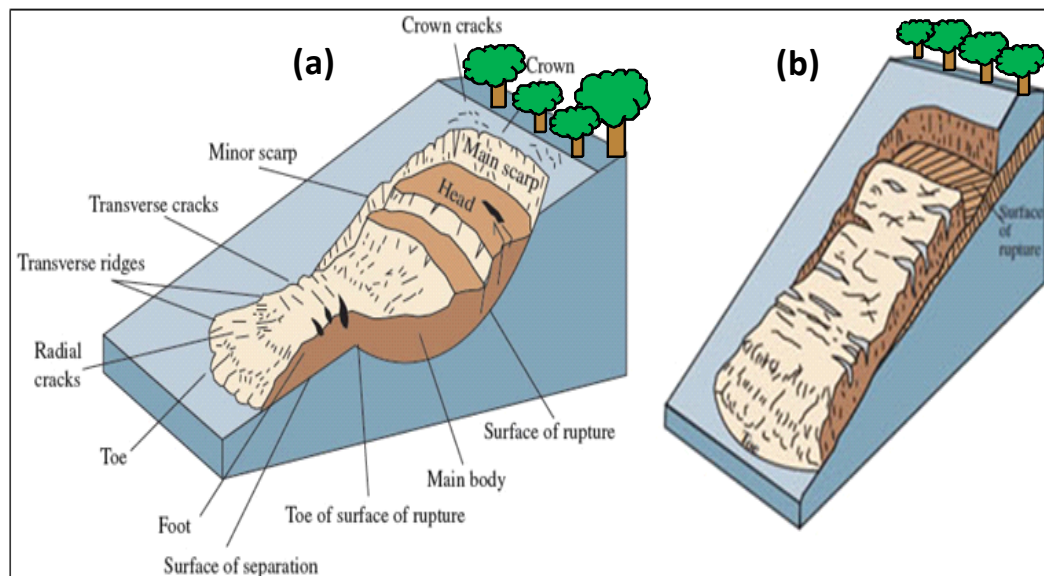

Fig. 4 Description of typical landslide types in the Kayangan catchment area: (a) slump and (b) transitional slide.

rotational movements in a slide and

observation path number 432, and an off-nadir angle

34.3º. The spatial and temporal baseline information of phenomena (Tralli, *et al.,* 2003). Since then, the method
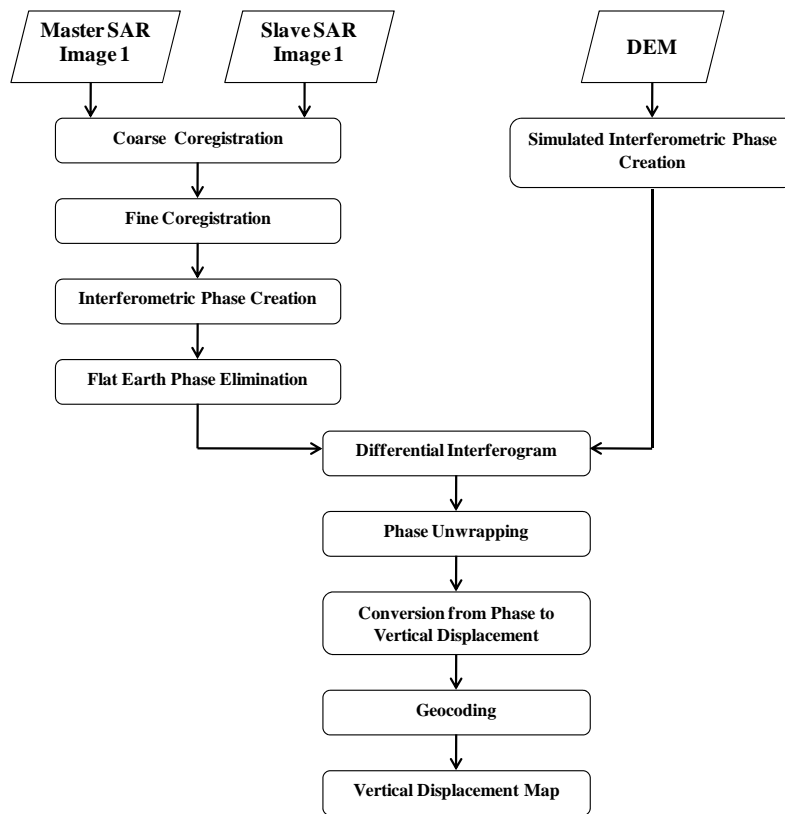

Fig. 5 Flowchart of DInSAR data processing.

each pair is listed in **Table 1.**

There are two kinds of resolution in the DInSAR results, namely the spatial resolution and deformation resolution. Spatial resolution of ALOS PALSAR is varying depending on the observation modes: for fine beam single (FBS) mode, the maximum resolution in the range direction is 7 m. The resolution in azimuth direction depends on the number of looks during processing: for example, ALOS PALSAR has azimuth resolution of 3.125 m and two looks lead to the maximum resolution of 7 m. Deformation resolution depends on the wavelength of the sensor. Short wavelength gives better resolution in some cases. In the case of ALOS PALSAR, the wavelength is 23.6 cm, leading to the typical deformation resolution of 11.6 cm.

Data Processing and Software

DInSAR analysis is implemented for two radar images obtained at different acquisition times. The phase information contained in eachSAR image is examined to derive the local topography (InSAR) or to determine and estimate the ground displacement that has happened between the two acquisitions (DInSAR) (Raucoules *et al.*, 2007). The DInSAR technique has been used since 1995 to detect surface deformation related to volcanoes

has also been applied to the analysis of landslide events (Strozzi *et al.*, 2005, Westen *et al.*, 2008, Cascini *et al.*, 2009). The phase difference between an InSARdata pair can be given as

$$\Phi_{Int} = \Phi_{disp} + \Phi_{topo} + \Phi_{atm} + \Phi_{noise} + \Phi_{flat} \qquad (1)$$

where ϕ_{disp} is the phase due to the surface deformation, ϕ_{topo} is the phase due to topographical height, ϕ_{atm} is the phase due to atmospheric effect, ϕ_{noise} the phase due to noise from the radar device, ϕ_{flat} the phase due to error associated with the assumption of the ideally flat earth terrain (Rosen *et al.,* 2000). In the procedure of extracting surface displacement, the topographic (ϕ_{topo}) and flat earth (ϕ_{flat}) phase differences should be eliminated using the DEM data coupled with accurate satellite orbital data (Bayuaji *et al.,* 2010 and 2012). The result of this phase is generally called DInSAR, which estimates the surface displacement in the slant-range direction (Δs). The surface displacement in the vertical direction, Δz, can be expressed as:

$$\Delta z = \Delta s \cos \theta \qquad (2)$$

Here DInSAR processing has been performed on four different ALOS PALSAR level 1.0 data from different acquisition years of 2007–2009 with the JAXA/SIGMA SAR processing software (Shimada, 1999). The flowchart of data processing is illustrated in **Fig. 5**. After image coregistration, DInSAR inter-ferogram is generated from each data pair. These DInSAR images are filtered using Goldstein and Werner filter with preconditioned conjugate gradient (Singhroy & Molch, 2004). Then, the phase unwrapping process is implemented to recover the information on the ground deformation along the slant-range direction. In the case of ALOSPALSAR, the wavelength is 23.6 cm (L-band) and hence, each cycle in interferogram represents ground deformation of 11.8 cm. Finally all images are geocoded by conducting cubic convolution using Universal Transverse Mercator (UTM) transformation and by resampling the DInSAR data to 12.5 m resolution.

We processed four SAR images recorded on the ascending mode with single HH polarization. Interpretations of change detection and thematic designation are conducted over the study area to construct a landslide susceptibility map, with the surface displacement distribution from the DInSAR analysis. Using a GIS platform (ArcMap GIS 9.3 and ENVI 4.8 software), all spatial data layers such as landcover, structure, slope and geology data as well as DEM including field observation data are composed to form a GIS-based landslide inventory database.

Our field observations of the landslide sites were conducted in 10 February 2009 to observe landslide locations with their dimensions. Also, GPS measurements were made to detect locations that might be triggering slides in the future. In **Fig. 6**, nine landslide locations are indicated on the relief map of the Kayangan catchment area. **Table 2** lists the observed length, displacement, and volume data from our GPS measurements. Landslide dimension of Kayangan area can be measured by several parameter, i.e. length of landslide (L), Surface displacement (D), and volume of landslide mass.

Table 2 Landslide dimension (length L, displacement D, and volume V) for the nine points in Fig. 5 based on the GPS Measurement.

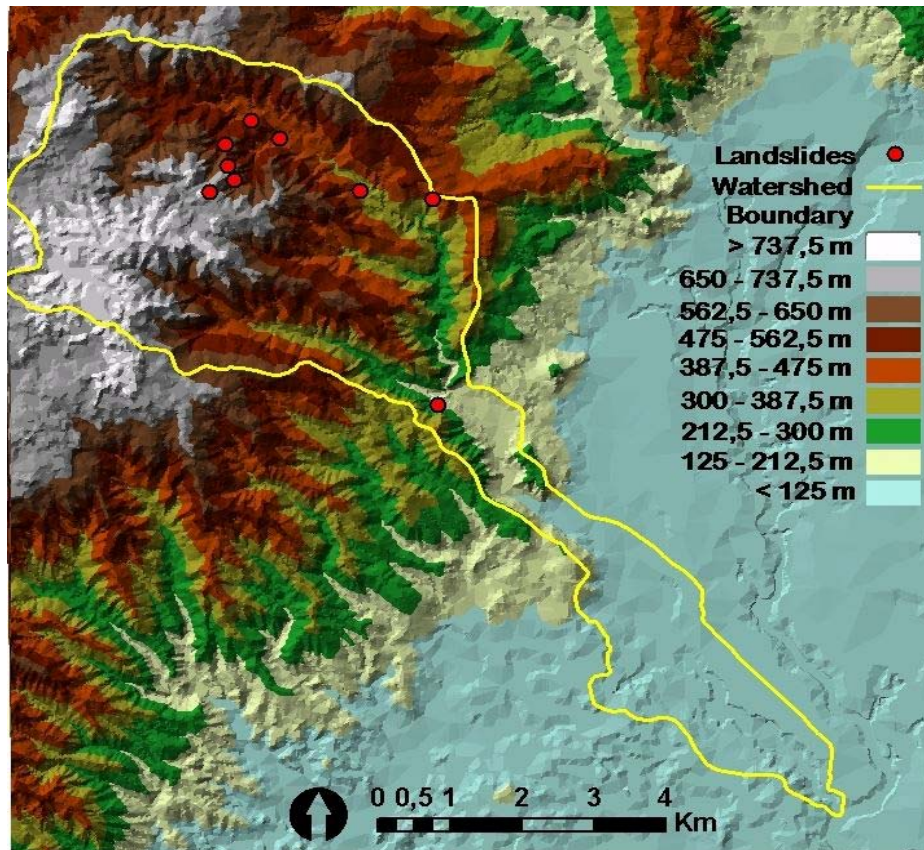| Location	L (m)	D (m)	V (m^3)
Point 1	100	70	2.063×10^5
Point 2	47.4	50	920.3
Point 3	45.6	15.2	8858
Point 4	35	15	4000
Point 5	25	21.3	990.2
Point 6	25.3	12.3	3310
Point 7	18	3	1036
Point 8	16.63	5.1	572.1
Point 9	16	11.2	249.6

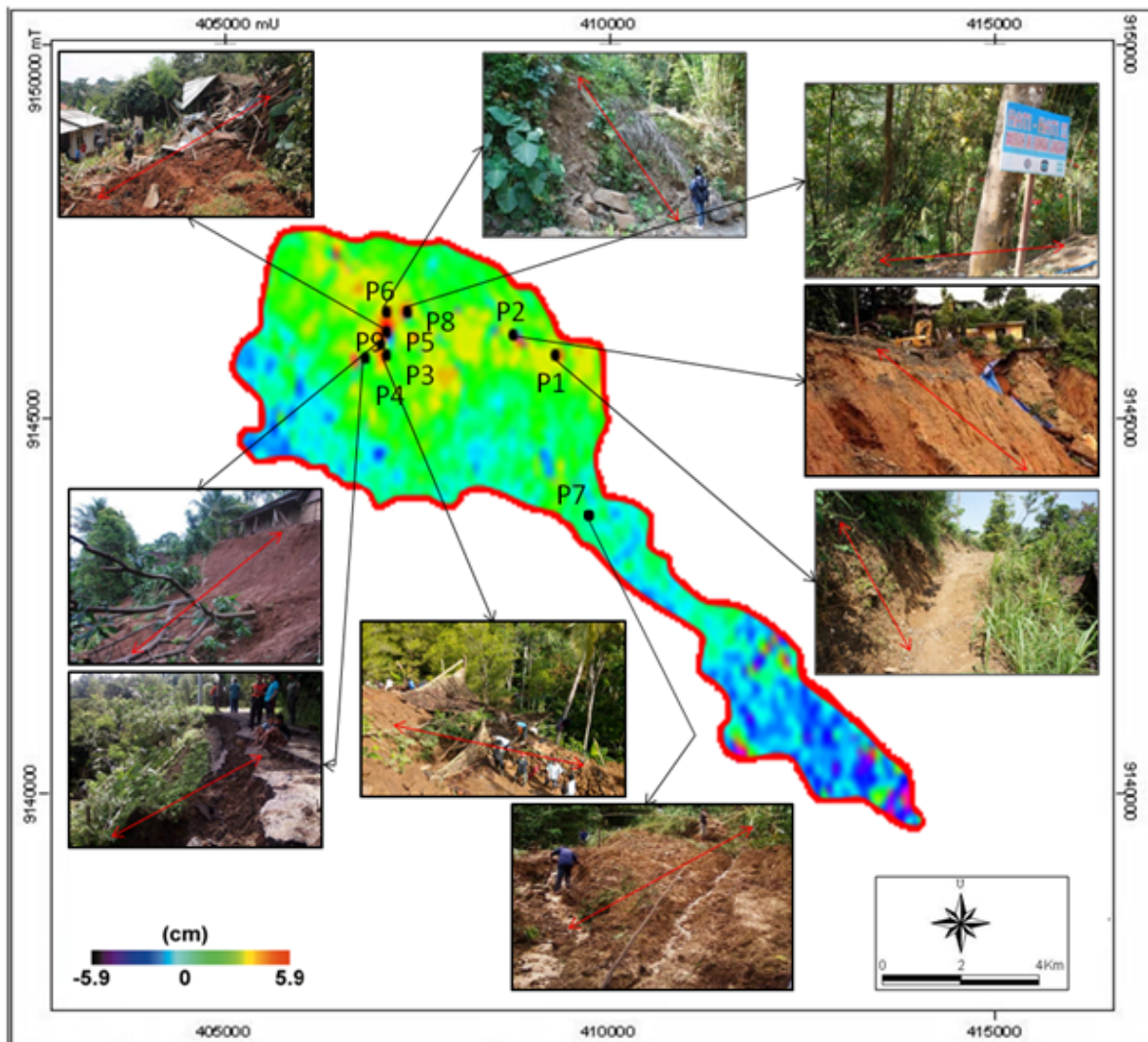**Fig. 6** Relief mapping of the study area with the spatial distribution of landslide events.

Fig. 7 DInSAR image with landslide locations and GPS positions from the field survey.

Landslide Location Inventory and Mapping

In order to achieve the present research goal, three steps of landslide detection using DInSAR techniques were performed: (1) landslide inventory and mapping; (2) preparation of terrain parameter maps; (3) analysis of the relation between landslide distribution and terrain parameter maps. Landslide inventory and mapping have been performed by utilizing various sources of data. The information concerning the type, length and width of landslide bodies was also considered in the data base.

Terrain parameter maps were obtained from various data sources. The lithological map was constructed from existing geological maps (1:50,000) (Rahardjo *et al.*, 2005). The slope map was obtained from a digital topographical map delivered by the National Agency of Survey and Mapping (1:25 000) (Bakosurtanal, 1997). To obtain the slope map and elevation map, a raster based DEM had been built by applying kriging interpolation using ILWIS software version 3.4. Drainage network, landuse map and road network map

were obtained directly from an existing digital map (Bakosurtanal, 1997). Buffer analysis was applied to classify the distance between roads and drainage network. Six classes of distances are used in this research, namely, 0–25 m; 25–50 m; 50–75 m; 75–100 m; 100–125 m; 125–150 m and > 150 m. Buffer analysis is employed to study the contribution of drainage and road networks to landslide occurrence. Spatial analysis of landslide distribution is conducted by overlaying the landslide distribution map on each terrain parameter map separately.

RESULTS AND DISCUSSION

Landslide Spatial Distribution

The DInSAR image pair of 2007−2008 shows an average linear movement of 22.5 cm around the landslide area (**Fig. 6**). Ground validation using high resolution differential GPS from the field also supports this interpretation of the DInSAR image. From ground
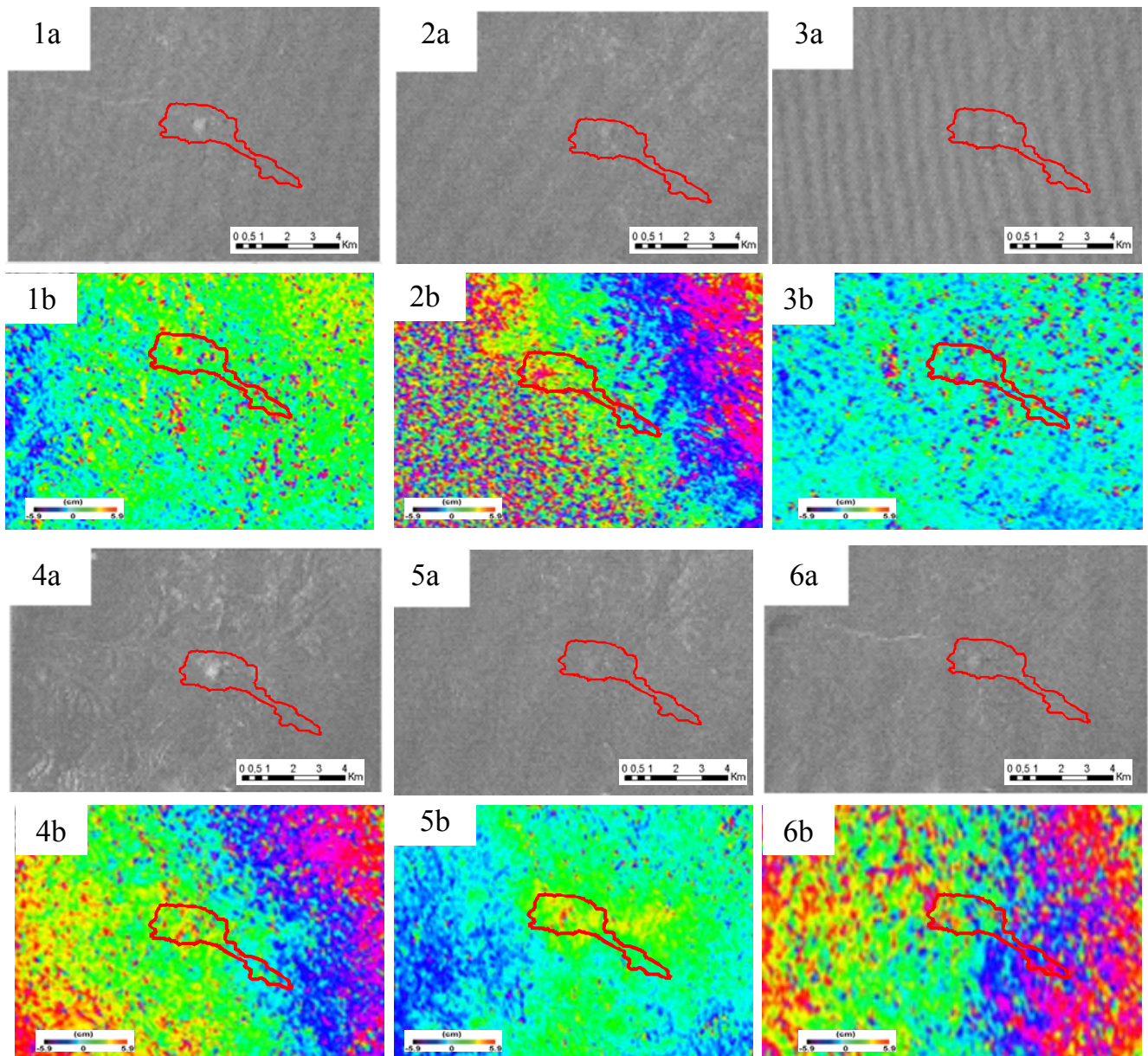
Fig. 8 ALOS PALSAR DInSAR Images: (a) coherence image for each of the six pairs of DInSAR result. Red lines indicate the affected areas, and (b) DInSAR images for the six different pairs: (1) 100807/120506, (2) 120508/120808, (3) 100807/120808, (4) 100807/150809, (5) 120808/150809, and (6) 120508/150809.

survey monitoring, we obtained the GPS locations of the landslides. Overlaying these points on the DInSAR imagery allows us to confirm the throne and the head of the landslides (**Fig. 7**). The image analysis shows that there is a slight deformation along the slope of the potential landslide in Point 1 area 409385 and 9146733 on UTM coordinate.

On the basis of the GIS data processing, visual delineation of the PALSAR DInSAR image overlaid with vector data shows that an area of approximately 0.33 km^2 has been affected at the upper part of Kayangan catchment. Significant mass movement prior to the landslide was detected by field observation in Kayangan catchment on 10 February 2009. On the other hand, the SAR processing using SIGMASAR yielded coherence images for each level 1.0 data of ALOS/PALSAR as shown in **Fig. 8**. Generating DInSAR images requires a pair of different acquisition images. Among the six pairs being processed, only two pairs, namely the pair images of August 2008/August 2007 and August 2009/August 2007, have shown reasonably good coherence (**Figs 8, 3b and 4b**). Based on the theory, coherence in DInSAR images is partly caused by the baseline of the two different acquisition times of the satellite observations. **Table 1** shows the parameters of the processed data pairs based on the observations in August 2007, May 2008, August 2008, and August 2009. The August 2008 /August 2007 and August 2009/August 2007 pairs have perpendicular baseline distances of 230.14 and 92.19 m, respectively.
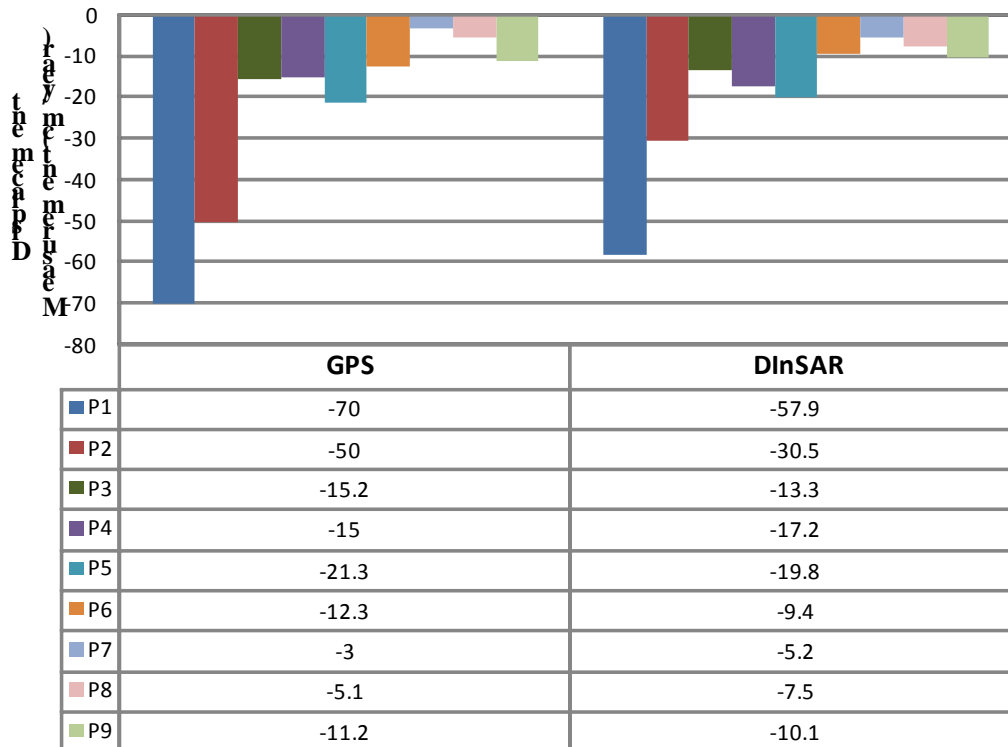
	GPS	DInSAR
■ P1	-70	-57.9
■ P2	-50	-30.5
■ P3	-15.2	-13.3
■ P4	-15	-17.2
■ P5	-21.3	-19.8
■ P6	-12.3	-9.4
■ P7	-3	-5.2
■ P8	-5.1	-7.5
■ P9	-11.2	-10.1

Fig. 9 Displacement measurement takenfrom the GPS measurement on 10 February 2009 and the maximum displacement from the DInSAR result between 10 August 2007-15 August 2009.

Beside this baseline factor, the coherence is also influenced by the atmospheric condition during theimage acquisition, such as heavy rainfall.

The result of GPS measurement conducted by file survey in 10 February 2009 also indicated landslide occurrences at all nine points. **Figure 9** shows the values of surface displacement derived from the GPS measurement conducted on 10 February 2009. All of the results of GPS measurement at nine locations (P1-P9) indicated the occurrence of landslide. The maximum surface displacement calculated from the DInSAR results, on the other hand, were in a range from -5.2 to -57.9 cm/year. **Figure 9** shows that the largest land subsidence occurred at P1, as indicated in both the GPS and DInSAR measurements.

Terrain Parameters Spatial Distribution

Nine landslide occurrences detected by DInSAR technique and fieldwork observation were mapped in the whole area of Kayangan catchment. Most of the landslides were situated on the upper and middle zone of the study area. In the lower part of the study area, on the other hand, landslides were not detected due to flat terrain morphology. Based on our fieldwork data, two types of landslides were indentified, i.e. slide type and slump type (see **Fig. 4**). Landslide that occurred at P6 was slump type while those at P1-P5 and P7-P8 were slide type.

The following six terrain parameters are mapped in the study area (**Fig. 10**): (a) elevation, (b) slope, (c) distance to stream network, (d) geology, (e) landuse, and (f) distance from road. The study area is dominated by elevation range below 100 m which is distributed in the southern part of Kayangan catchment (6.25 km^2) while the area with elevation range 200-300 m coversonly a small area (1.86 km^2) (**Fig. 10a**). Slope classification indicates that the largest proportion of slope inclination is 30–40° which is distributed across an area of 11.47 km^2 in the lower part of the drainage basin (**Fig. 10b**).

According to the buffer map of stream networks (**Fig. 10c**), the study area is dominated by the distance more than >150 m from stream networks (10.54 km^2) while the area with the distance 125-150 m covers only a small area (2.80 km^2). All of the landslide locations are in Kebubotak formation (25.96 km^2). **Figure 10d** shows the landslide locations on the geology map of Kayangan catchment. Regarding the type of landuse (**Fig. 10e**), the area is dominated by mixed garden which is distributed on a wide range of terrain conditions (17.74 km^2). Mixed garden consists of cloves, bamboos, coconut trees and other types of hard trees. This landuse is usually associated with settlement which covers 4.55 km^2. Agricultural activities are also dominant in Kayangan catchment, represented by the surface of rice field (5.5 km^2) and dryland agriculture

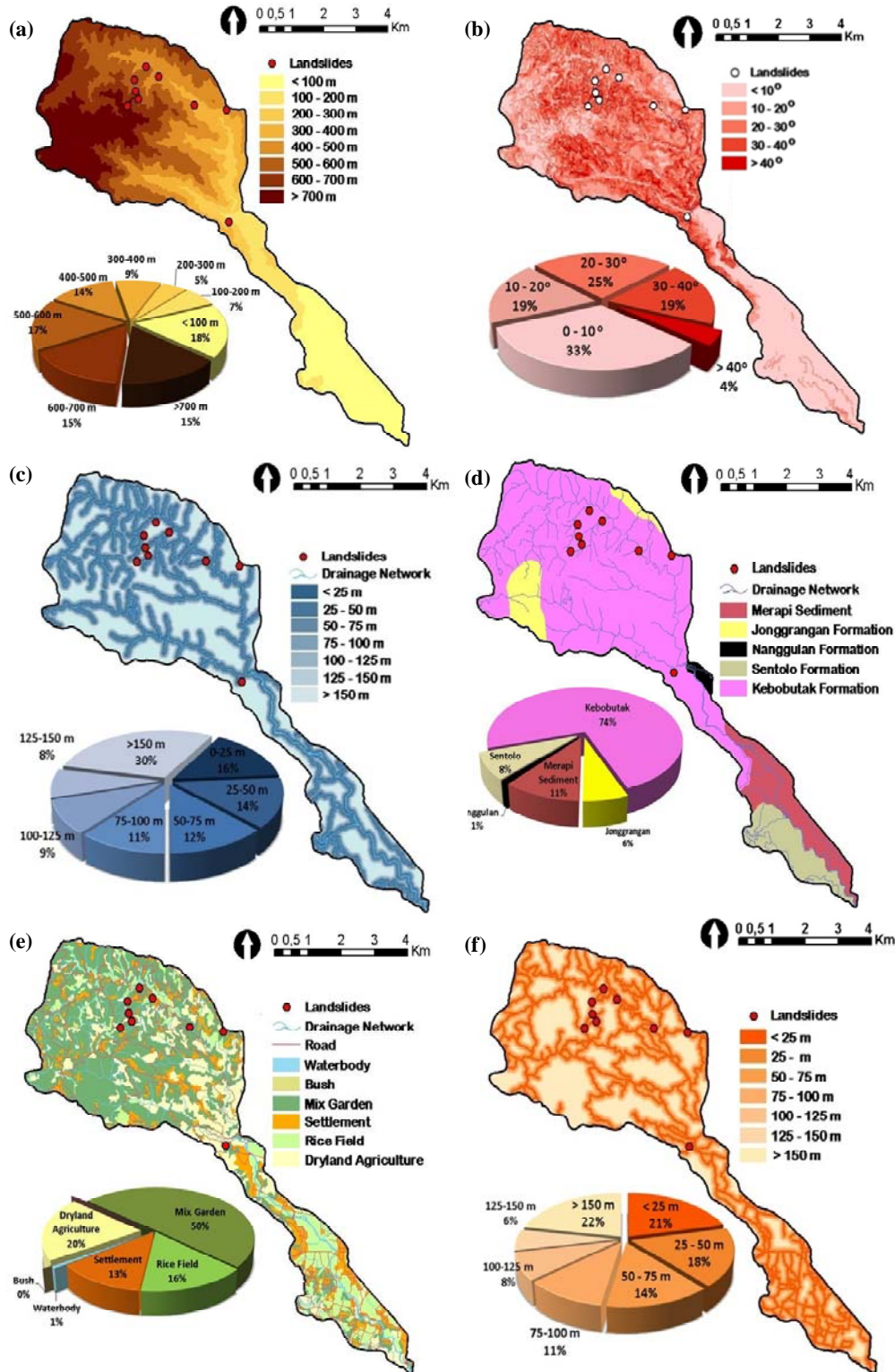(7.12 km^2). **Figure 10f** shows the road network. The

Fig. 10 Terrain parameter maps of Kayangan catchment with landslide locations and pie charts showing the area proportion of each terrain parameter value: (a) elevation, (b) slope, (c) distance to stream network, (d) geology, (e) landuse, and (f) distance from road.

study area has relatively well-conditioned roads even in the village area. Buffer class of road networks shows that landslide sites are located mainly at locations having a distance of > 150 m (7.7 km^2).

Landslide and Terrain Parameters Analysis

From the present data analysis of DInSAR and fieldwork measurements, it has been found that only one lithology type, namely Kebobutak Formation (25.96

km²) had been subjected to landslide occurrence. This land type has andesitic breccias, tuff, lapili tuff, agglomerate and andesitic lava flows. Thus, it is likely that strong weathering and fracturing of the andesite and andesitic breccia might have played an important role on landslides predisposition.

The relationship between landslide occurrence and slope (**Fig. 11c-d**) shows that steeper slopes have greater landslide frequency up to slope steepness of 30 – 40°. Concentrated distributions of landslide sites can be found on moderately steep terrain, ranging from 30° to 40° (0.75 events per km²). However, inverse correlation has been seen between landslide occurrence and slope

steepness when the slope angle is more than 40°.

Theoretically, as the slope angle increases, the shear stress in the soil or other unconsolidated material generally increases and the landslide probability increases (Lee & Pradan, 2006). Gentle slopes are expected to have low frequency of landslides because of generally lower shear stresses associated with low gradients. However, this case is not always applicable for all types of terrains. For example, in the present study area, several landslide incidents can be found on the gentle-to-moderate slopes (less than 20°), presumably due to the role of other factors disturbing slope stability such as human activities (Paudel *et al.*,
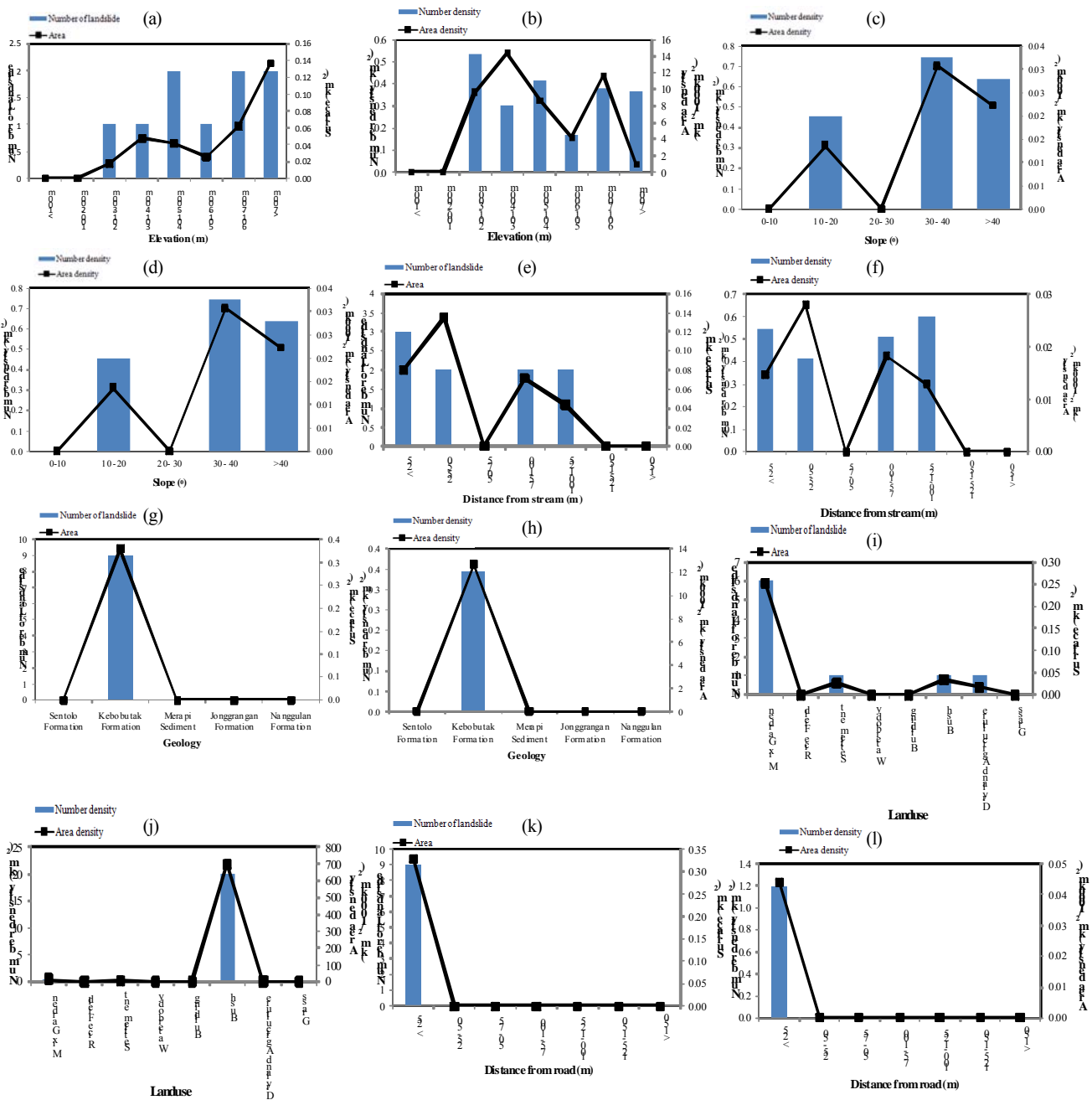

Fig. 11 Number of landslides, landslide area and lanslide density for (a, b) elevation, (c, d) slope, (e, f), distance from stream, (g, h) geology, (i, j) landuse, and (k, l) distance from road.

2000). Very steep slopes are sometimes absent from landslide activities because of the existence of resistant bedrocks and consolidated materials. These usually consist of non-arable land, leading to fewer influence of human activities.

Landslide distribution overlaid on elevation data (**Fig. 11a**) indicates a similar pattern. Landslide events increase significantly with increasing elevation up to 400 m, as depicted in **Fig. 11a,b**. Most of the landslides occurred in the elevation belt of 401-500 m. Number density and area density reached 0.41 events/km^2 and 8.67 km^2/1000 km^2, respectively. Below 400 m altitude, the landscape is gentler: it becomes steeper as elevation rises due to the appearance of andesitic rocks and presence of underlying pyroclastic bedrocks. The present results are consistent with those of Dai and Lee (2002) in Lantau Island, Hongkong, and Paudel *et al*. (2007) in Mt. Aso, Japan. At very high elevations, there are mountain summits that generally consist of weathered rocks, in which the influence of shear stress is much stronger. At intermediate elevations, however, slopes tend to be covered by unconsolidated materials like colluviums, which is more prone to slide.

The relationship between landslide frequency and stream network reveals that most of landslides are situated at distances less than 25 m from river (three events, which is equal to 0.54 events/km^2) (**Fig. 10e,f**). Number density in less than 25 m reached 14.52 km^2/1000 km^2. The landslide events occurred in the zone of 25−50 m, 75−100 m and 100−125 m from river. There is no apparent trend indicating decreasing of landslide frequency with the increasing distance from rivers. However, the landslide occurrence was the highest in the buffer zone less than 25 m, which indicates that most of bigger landslides are situated near the rivers. It is likely that this is due to the slope modification by gully erosion, which can influence the initiation of landslides. This result confirms previous research by Dai and Lee (2002) who found that as drainage line increases, the frequency of landslide generally decreases.

Analysis of landslide occurrence based on type of landuse shows that there are only four types of landuse that can lead to landslide occurrence, i.e., mixed garden, dryland agriculture, bush, and settlement (**Fig. 10i-j**). Mixed garden is the landuse most susceptible to landslide (9 events) with the area and number density reaching 14.23 km^2/1000 km^2 and 0.34 events/km^2, respectively. However, the highest number and area density of landslides have been identified in bush with the values of 20 events/km^2 and 700 km^2/1000 km^2. Since both mixed vegetation and bush can be categorized into manmade terrain, human contribution underlies higher occurrence of landslides.

In order to assess such human contribution, we have further analyzed landslide frequency in relation to the distance from road networks (**Fig. 10k,l**). The majority of landslides occurred in zones with distances less than 25 m from nearby road network. Three landslide events have been mapped in this area with the number density and area density of 0.01 events per km^2 and 5.47 km^2/1000 km^2, respectively. This suggests that road networks play important role in landslide initiation, presumably by undercutting and removing the toe of slopes for constructions of roads or houses. Due to land limitation and low risk perception, for instance, local people tend to build their houses on step slopes as shown in **Fig. 12**.

CONCLUSIONS AND FUTURE WORK

In this research, we have demonstrated the capability of remote sensing technique for monitoring landslide hazard in Kayangan catchment of Kulon Progo, Yogyakarta, Indonesia. We have implemented DInSAR analysis of ALOS PALSAR image to estimate surface displacement of landslides in the study area. The L-band data of ALOS PALSAR have been successfully used to map active landslides over an area of 0.33 km^2 by 28.49 km^2 in the upper and middle parts of Kayangan catchment. The maximum surface displacement rates are 57.9 cm/year (P1), 30.5 cm/year (P2) and 19.8

Fig. 12 Several houses on the step slope in Kayangan catchment.

cm/year (P5). Thus, the present result shows that the DInSAR analysis of ALOS PALSAR data are able to detect surface deformation in sub centimeter. Furthermore, the DInSAR result can also be used to generate a hazard map of the area, since the L-band data show good terrain information irrespective of vegetation coverage. Based on **Fig. 10e**, the surface deformation in landslide area occurred in separate regions with different types of landuse such as mixed garden, dryland agriculture, and terrace rice.

The L-band DInSAR results have constructed good fringe patterns in either short or long time duration. The short time duration was found in pair May 2008/August 2008 with temporal baseline 12 week and the long time duration with temporal baseline 96 week in pair August 2007/August 2009. This ability is beneficial to create temporal landslide monitoring map for further studies. Continuous information of landslide hazard estimation will be useful for the development of catchment areas, as one of the important factors for planning and construction works.

The terrain parameters have different levels of contribution to land sliding which were indicated by density and frequency of landslide in each parameter. Comprehensive analysis of landslide and terrain parameter has revealed physical-natural factors (geology, slope, elevation, and distance to networks) and human activities that contribute to landslide occurrence in the study area. We found that human activities play an important role in landslide acceleration, particularly through slope cutting for houses and road construction.

The continuation of DInSAR analysis based on ALOS PALSAR data can be combined with other studies to elucidate the cause of local landslide phenomenon and appropriate ideas for its prevention. We have found that DInSAR technique provides effective and low cost disaster monitoring process compared to conventional ground survey. In case disaster monitoring by detailed ground survey is inevitable, DInSAR technique can be applied as preliminary observation process since DInSAR result is able to give better spatial perspective rather than point perspective. This result is able to give useful information for disaster mitigation actions.

Further works must be carried out to validate the accuracy of the DInSAR image as it is still an estimation result. Validation with ground checked must also be carried out. Applying DInSAR method with TerraSAR-X images will be done a better result considering ALOS PALSAR has better accuracy for thedevice specifications compared to ALOS PALSAR. The next research will be created a statistical analysis to make susceptibility map as landslide inventory based on DInSAR image processing of study area.

REFERENCES

Abidin, H.Z., Andreas, H., Djaja, R., Darmawan, D. & Gamal, M. (2008) *Land subsidence characteristics of Jakarta between 1997 and 2005, as estimated using GPS surveys*. GPS Solutions, Springer Publisher. **12**(1):23–32.

Bakosurtanal (The National Agency of Survey and Mapping). (1997) *Peta Rupa Bumi* 1:25.000. Cibinong, Indonesia.

Bayuaji, L., Sumantyo, J.T.S. & Kuze, H. (2010) *ALOS PALSAR D-InSAR For land subsidence mapping in Jakarta, Indonesia*. Can. J. Remote Sensing. **36**(1):1–8.

Bayuaji, L., Putri, R.F. & Sumantyo, J.T.S. (2012) *Combination of L, C and X-band SAR data for continuous monitoring of land deformation in urban area by using DInSAR technique*. Proceeding IEICE Technical Report SANE, 77-82.

Badan Pusat Statistik (BPS). (2008) *Kabupaten Kulon Progo Dalam Angka 2008*. BPS, Yogyakarta.

Cascini, L., Fornaro,G., & Peduto, D. (2009) *Analysis at medium scale of low-resolution DInSAR data in slow-moving landslide-affected areas*. ISPRS Journal of Photogrammetry and Remote Sensing. **64**:598-611.

Chini, M., Bignami, C., Stramondo, S., & Pierdicca, N. (2008) *Uplift and subsidence due to the 26 December 2004 Indonesia Earthquake detected by SAR data*. International Journal of Remote Sensing, **29**:3891-3910.

Colesanti, C., Mouelic, S.L., Bennani, M., Raucoules, D., Carnec, C., & Ferretti, A. (2005) *Detection of mining related ground instabilities using the Permanent Scatterers technique a case study in the east of France*. International Journal of Remote Sensing., **26**:201-207.

Colesanti, C., & Wasowski, J. (2006) *Investigating landslides with space-borne Synthetic Aperture Radar (SAR) interferometry*. Engineering Geology ,(88):173–199.

Curlander, J.C., & McDonough, R.N., (1991) *Syntetic aperture radar: systems and signal processing*. Wiley-Interscience, Toronto, Ont: 672.

Dai, F.C., & Lee, C.F. (2002*) Landslide characteristic and slope instability modeling using GIS, Lantau Island, Hongkong*. Geomorphology (42):213-228.

Dong, Y, Li, Q., Dou, A., & Wang, X. (2010) *Disaster Mapping from Medium Spatial Resolution ALOS PALSAR Images*. Proceeding of International Geoscience and Remote Sensing Symposium (IGARSS). Honolulu Hawaii, USA, 25-29 July 2010, 2167-2170.

Hadmoko, D.S., Lavigne F., Gonez C., Sartohadi J., & Daryono, N. (2008) *Spatio-temporal Characteristic of Landslides in Java and Their Factors*. Paper presented on the International Conference on Geomorphology. Yogyakarta, Indonesia, 25-29 Agustus 2008.

Ignasius & Nursa'ban, M. (2012) *Kajian Tingkat Kerentanan Longsor Lahan Sub DAS Kayangan Kabupaten Kulon Progo Provinsi Daerah Istimea Yogyakarta (Landslide Vulnerability Assessment in Kayangan Catchment, Yogyakarta Special Province)*. Thesis, UNY, Yogyakarta. Available in: http://library.fis.uny.ac.id/index.php?p=show_detail&id=1022. Accesed in: 26 September 2013.

Lee, S., & Pradan, B. (2006) *Probabilistic landslide hazards and risk mapping on Penang Island, Malaysia*. Journal of Earth System Science.**115**(6):661-672.

Lucas, RM., Moghaddam, M., & Cronin, N. (2004)*Microwave scattering from mixed-species forests, Queensland, Australia.* IEEE Transactions on Geoscience and Remote Sensing. **42**: 2142–2159.

Massonnet, D., Rossi, M., Carmona, C., Adragna, F., Peltzer, G., Fiegl, K., & Rabaute, T. (1993) *The displacement field of the Landers earthquake mapped by radar interferometry.* Nature. **364**:138–142.

Matternicht, G., Hurni., & Land Gogu, R. (2005) *Remote sensing of landslides: An analysis of the potential contribution to geo-spatial systems for hazard assessment in mountainous environments.* Remote Sensing of Environment, Elsevier ltd. **124**: 348-359.

Ozawa, S., Murakami, M., Fujiwara, S., & M., Tobita, M. (2012) *Synthetic aperture radar interferogram of the 1995 Kobe earthquake and its geodetic inversion.* Geophysical Research Letters. **24**:2327–2330.

Paudel, P.P., Omura, H., Kubota, T., & Inoue, T. (2007) *Spatio temporal patterns of historical shallow landslides in a volcanic area, Mt. Aso, Japan.* Geomorphology. (88):21-33.

Putri, R.F., Aminuddin, A., Sri Sumantyo, J., & Kuze, H. (2013) *Landlside HAZARD Detection Using ALOS PALSAR DinSAR Technique: Study Case Kayangan Catchment Area, Yogyakarta, Indonesia.* Proceeding of the 34th Asian Conference on Remote Sensing 2013. Bali, October 20-24, 2013.

Rahardjo, W., Sukandarrumidi., & Rosidi, H. M. D. (1995) *Peta Geologi Lembar Yogyakarta, Jawa.* Pusat Penelitian dan Pengembangan Geologi, Bandung.

Raucoules, D., Colesanti, C. & Carnec, C. (2007) *Use of SAR interferometry for detecting and assessing ground subsidence.* Comptes Rendus Geoscience. **339**(5), 289–302.

Riedel, B., & Walther, A. (2008) *InSAR processing for the recognition of landslide.*Advances in. Geosci. (14), 189–194.

Rosen, P.A., Hensley, S., Joughin, I.R., Li, F.K.,Madsen, S.N., Rodriguez, E. & Goldstein, R.M. (2000) *Synthetic aperture radar interferometry.* Proceedings of the IEEE. **88**(3): 333–382.

Rosenqvist, A., Shimada, M., Ito, N., & Watanabe, M. (2007) *ALOS PALSAR: A Pathfinder Mission for Global-Scale Monitoring of the Enviuronment.* IEEE Transaction on Geoscience and Remote Sensing, **45**(11), 3307-3316.

Rott, H., Scheuchl, B., Siegel, A., & Grasemann, B. (1999) *Monitoring very slowslopemovements by means of SAR interferometry: A case study from a mass waste above a reservoir in the Ötztal Alps, Austria.* Geophysical Research Letters. **26**:1629–1632.

Singhroy,V., & Molch, K. (2004) *Characterizing and monitoring rockslides from SAR Techniques.* Advances in Space Research. (33):290-295.

Squarzoni, C., Delacourt, C., & Allemand, P. (2003) *Nine years of spatial and temporal evolution of the La Vallette landslide observed by SAR interferometry.* Engineering Geology. **68**:53–66.

Strozzi, T., Farina, P., Corsini, A., Ambrozi, C., Thuring, M., Zilger, J., Wiesmann, J., Wegmuller, U., & Werner, C. (2005) *Survey and monitoring of landslide displacements by means of L-band satellite SAR Interferometry.* Landslides. **2**:193–201.

Tralli, D.M. Blom, R. G., Zlotnicki, V., Donnellan A. & Evans, D. L. (2005) *Satellite remote sensing of earthquake, volcano, flood, landslide and coastal inundation hazards.* ISPRS Journal of Photogrammetry and Remote Sensing. **59**(4), 185-198.

Tsuji, T., Yamamoto, K., Matsuoka, T., Yamada, Y., Onishi, K., Bahar, A., Meilani, I., & Abidin, H.Z. (2009) *Earthquake fault on the May 2006 Yogyakarta earthquake observed by SAR Interferometry.* Earth Planet Space. **61**:e29-e32.

U.S. Geological Survey. (2006) *Magnitude 6.3 – JAVA, INDONESIA, The record of earthquake in Yogyakarta, Central Java.* Available in:(http://earthquake.usgs.gov/earthquakes/eqinthenews/2006/usneb6/ Accessed in 3 July 2013.

Walter, T.R., Wang, R., Luehr, B.G., Wassermann, J., Behr, Y., Parolai, S., Anggraini, A., Gunther, E., Sobiesek, M., Grosser, H., Wetzel, H.U., Milkereit, C., Sri Brotopuspito, P.J.K., Harjadi, P., & Zschau, J. (2008) *The May 2006 magnitude 6.4 Yogyakarta earthquacke south of Mt. Merapi Volcano: did lahar depsits amplfy ground shaking and thus lead the disaster?.* Geochem. Geophys. Geosyst, Wiley, USA.

Westen, C.J, Castellanos, E., & Kuriakose, S.L. (2008) *Spatial data for landslide susceptibility, hazard, and vulnerability assessment.* Engineering Geology. **102**:112-131.

Zaruba, Q., & Mencl, V. (1982) *Landslide and Their Control.* Elsevier. 110-120.